International Journal of Creative and Open Research in Engineering and Management
ISSN: **3108-1754 (Online)**
Volume 02 Issue 05 May-2026 | Impact Factor: 3.5

Anisotropic Mechanical Behaviour of Selective Laser Melted AlSi10Mg Alloy Fabricated at Different Build Orientations

Sagar N. Jadhav[1], J. B. Shaikh[2], S. C. Borse[3], D.U. Gopekar[4] ,K.B.Kolhapure

Department of Mechanical Engineering,

Deogiri Institute of Engineering and Management Studies,

Chhatrapati Sambhajinagar, Maharashtra, India

*Corresponding Author Email: jawedshaikh086@gmail.com, sagarjadhav12052000@gmail.com

How to Cite this Article:

Jadhav, S. N., Shaikh, J. B., Borse, S. C., Gopekar, D. & K.B.Kolhapure, (2026). Anisotropic Mechanical Behaviour of Selective Laser Melted AlSi10Mg Alloy Fabricated at Different Build Orientations. International Journal of Creative and Open Research in Engineering and Management, 02(05). https://doi.org/10.55041/ijcope.v2i5.849

https://doi.org/ 10.55041/ijcope.v2i5.849

Abstract

Additive manufacturing (AM) is increasingly used for producing lightweight and complex metal components with reduced material waste and shorter production time. Selective laser melting (SLM) is widely employed for manufacturing AlSi10Mg alloy parts for aerospace and automotive applications. In the present work, the influence of build orientation on the microstructure and mechanical properties of SLM-fabricated AlSi10Mg alloy was investigated. Samples were fabricated at 0°, 45°, and 90° orientations and analysed using microstructural, density, hardness, and tensile characterization techniques.

The microstructures revealed characteristic melt pool patterns and laser scan tracks formed during the SLM process. Relative density values ranged from 97.3% to 98.27%, while hardness values varied between 126–128 HV. Tensile testing demonstrated clear anisotropic behaviour with variation in build orientation. The 45° specimens exhibited the highest elongation of 7.4%, whereas the 90° specimens achieved the maximum ultimate tensile strength of 450 ± 6 MPa. The observed variations were mainly attributed to differences in melt pool overlap and interlayer bonding. The results confirm that build orientation significantly influences the mechanical performance of as-built SLM AlSi10Mg alloy.

Keywords: *Selective laser melting; AlSi10Mg; Build orientation; Anisotropy; Mechanical properties; Additive manufacturing.*

Introduction

Selective laser melting (SLM) is a powder bed fusion-based metal additive manufacturing technique in which metallic powder is selectively melted using a high-energy laser according to computer-aided design (CAD) data. The process enables fabrication of near-net-shape components with complex geometries and high dimensional accuracy [1,2]. Due to its ability to reduce material waste and produce topology-optimized structures, SLM has gained significant attention in aerospace, automotive, biomedical, and energy industries [2].

The quality and mechanical performance of SLM-fabricated components are strongly influenced by processing parameters such as laser power, scan speed, hatch spacing, layer thickness, and scanning strategy [3]. These parameters affect melt pool behaviour, cooling rate, porosity formation, and residual stress development. Improper processing conditions may lead to defects including lack-of-fusion pores, balling, keyhole defects, and microcracks, which adversely affect component performance [4–6].

Among aluminium alloys, AlSi10Mg has attracted considerable interest due to its low density, high strength-to-weight ratio, good corrosion resistance, and excellent thermal conductivity [7]. However, processing aluminium alloys through SLM remains challenging because of their high thermal conductivity and laser reflectivity, which reduce laser absorption efficiency and influence melt pool stability [8]. Rapid solidification during processing may also promote oxide formation and gas entrapment, resulting in porosity and weak interlayer bonding [9].

Recent studies have reported that build orientation significantly influences the anisotropic behaviour of SLM-fabricated AlSi10Mg alloys [6,11,12]. Variations in build direction affect heat flow, grain growth, melt pool overlap, and residual stress distribution, leading to orientation-dependent changes in density, tensile strength, hardness, and ductility. Vertical specimens generally exhibit higher tensile strength, while horizontal orientations often show lower porosity and improved density [6,11,12].

Accordingly, the present study investigates the influence of build orientation on the density, porosity, hardness, microstructure, and tensile properties of as-built AlSi10Mg alloy fabricated by SLM without post-processing heat treatment. Tensile specimens were fabricated in XY-0°, 45°, and Z-90° orientations. The novelty of this work lies in the comparative evaluation of orientation-dependent mechanical behaviour and microstructural characteristics under identical processing conditions.

2. Experimental Procedure

The tensile specimens shown in Figure 1 were fabricated using an EOS EOSINT M280 selective laser melting system, a commercial selective laser melting machine operating with fixed processing parameters: 150 W laser power, 1000 mm/s scan speed, 50 µm hatch spacing, and 50 µm powder layer thickness. Four specimens were produced for each build orientation. Three specimens from each orientation were used for tensile testing, while the remaining specimen was sectioned for microstructural analysis. The samples were classified according to build orientation as XY-0° (Batch A), 45° (Batch B), and Z-90° (Batch C), as illustrated in Figure 1.

Figure 1 Build orientations of SLM-fabricated AlSi10Mg tensile specimens.

2.1 Characterization

Density measurements of the tensile specimens were carried out using the OHAUS EX244/AD densitometer based on the Archimedes principle, with ethanol used as the immersion medium. The specimens were subsequently sectioned, mounted, polished, and etched using Keller's reagent prior to microstructural examination with the Olympus Corporation BX51M optical microscope.

Hardness characterization was performed on the mounted specimens using a Zwick Roell Micro/Macro Vickers hardness tester. A load of 300 g was applied, and 20 indentations were made on each sample, with the average value reported. Tensile testing was conducted using a 20 kN Zwick Roell tensile testing machine in accordance with ASTM E8/E8M-16a standards to determine the tensile properties of the specimens. Gas atomized AlSi10Mg powder was used as the feedstock material for the selective laser melting (SLM) process. Gas atomization ensures near-spherical powder morphology, good flowability, and uniform particle packing, which are essential for achieving stable melt pool formation and consistent layer deposition during fabrication.

The powder particle size distribution was in the range of 20–63 μm, which is suitable for powder bed fusion-based additive manufacturing processes. The powder was supplied by a commercial SLM material. The powder was used in the as-received condition without any additional treatment. The chemical composition of the AlSi10Mg powder is presented in Table 1.

Table 1 The chemical composition of the AlSi10Mg powder

Element	**Si**	**Mg**	**Fe**	**Al**
wt.%	9–11	0.2–0.45	<0.55	Balance

3. Results and Discussion

3.1 Density and Porosity Analysis

The density and porosity results of the SLM-fabricated AlSi10Mg specimens produced with different build orientations are presented in Table 2. The measured densities for all orientations were comparable and consistent with the literature value of 2.67 g/cm³ reported for commercially manufactured AlSi10Mg alloys [3]. Among the investigated orientations, Batch A (XY orientation) exhibited the lowest porosity levels and consequently the highest relative density. In contrast, Batch C (Z orientation) showed the highest porosity content. Nevertheless, the porosity values ranged from 1.73% to 2.70%, corresponding to relative densities between 97.3% and 98.27%, which are comparable to previously reported as-built SLM AlSi10Mg components reported in the literature [4,6].

Although several studies have investigated the influence of build orientation on SLM-fabricated AlSi10Mg alloys, inconsistencies remain regarding the relationship between porosity evolution, melt pool morphology, and tensile behaviour in as-built conditions without post-processing treatment. Furthermore, comparative evaluation of density, microstructure, hardness, and tensile behaviour under identical processing conditions remains limited.

Table 2 Properties of SLM -produced sample in different orientations

Build Orientation	Density (g/cm³)	Porosity (%)	Relative Density (%)	Hardness (HV)
A (XY / 0°)	2.624 ± 0.023	1.73 ± 0.85	98.27 ± 0.85	127 ± 0.635
B (45°)	2.617 ± 0.014	2.00 ± 0.52	98.00 ± 0.52	128 ± 0.641
C (Z / 90°)	2.598 ± 0.032	2.70 ± 1.21	97.30 ± 1.21	126 ± 0.630

For clarity on the porosity results observed in table 2, the microstructures of the samples were analysed to determine the presence of pores on the internal surfaces of the samples.

3.2 Microstructural analysis

The scanning direction microstructures of the SLM samples produced in different orientations are presented in Figure 2. The images of Batch A at different magnifications (Figure 2a & d) show microstructures consistent with the laser scan pattern formed during the SLM process. This scale-like morphology has also been reported previously [1]. The scanning pattern sizes in Figure 2a were measured using ImageJ and were found to be 50–90 µm in height and 120–330 µm in width. At higher magnifications, Figure 2d shows the presence of cellular and dendritic growth within the grain structure. Similar cellular and dendritic microstructures have also been reported previously [1,4,17], which were attributed to eutectic silicon particles located along grain boundaries. The pores (dark regions corresponding to pores on the microstructure) in this sample were scattered and were not observed in all tracks. Previous studies on SLM-processed AlSi10Mg samples also reported different types of pores located at melt pool boundaries, resulting from entrapped gases, oxides, or evaporated powder particles [9,10].

The microstructures of Batch B samples (Figure 2b & e) also showed a laser scan pattern, although in this case the grains were oriented diagonally relative to the laser scan path. The scan pattern sizes were measured as 28–156 µm in height and 113–344 µm in width, and pores were observed on nearly every track including grain boundaries. Figure 2b & e showed dendritic growth near the boundaries and cellular growth within the structural morphology. The high cooling rate associated with SLM promoted refinement of the microstructure and limited the formation of coarse dendrites while promoting the formation of fine cellular microstructures [1,4,8].

A scale-like pattern similar to Batch A was also observed in Figure 2c & f for Batch C. The scan pattern sizes were measured as 50–135 µm in height and 140–248 µm in width. Pores were clearly observed in this structure, particularly in Figure 2c. These pores may have resulted from undissolved powder particles or insufficient overlap between scan tracks. Spherical pores are generally associated with trapped gases, oxides, or evaporated powder particles. Similar pore formation inside melt pools has also been reported previously [6]. The porosity observed in the microstructures is consistent with the porosity values obtained using the Archimedes method presented in Table 2, where the Z orientation exhibited the highest quantified porosity and visible pore concentration.

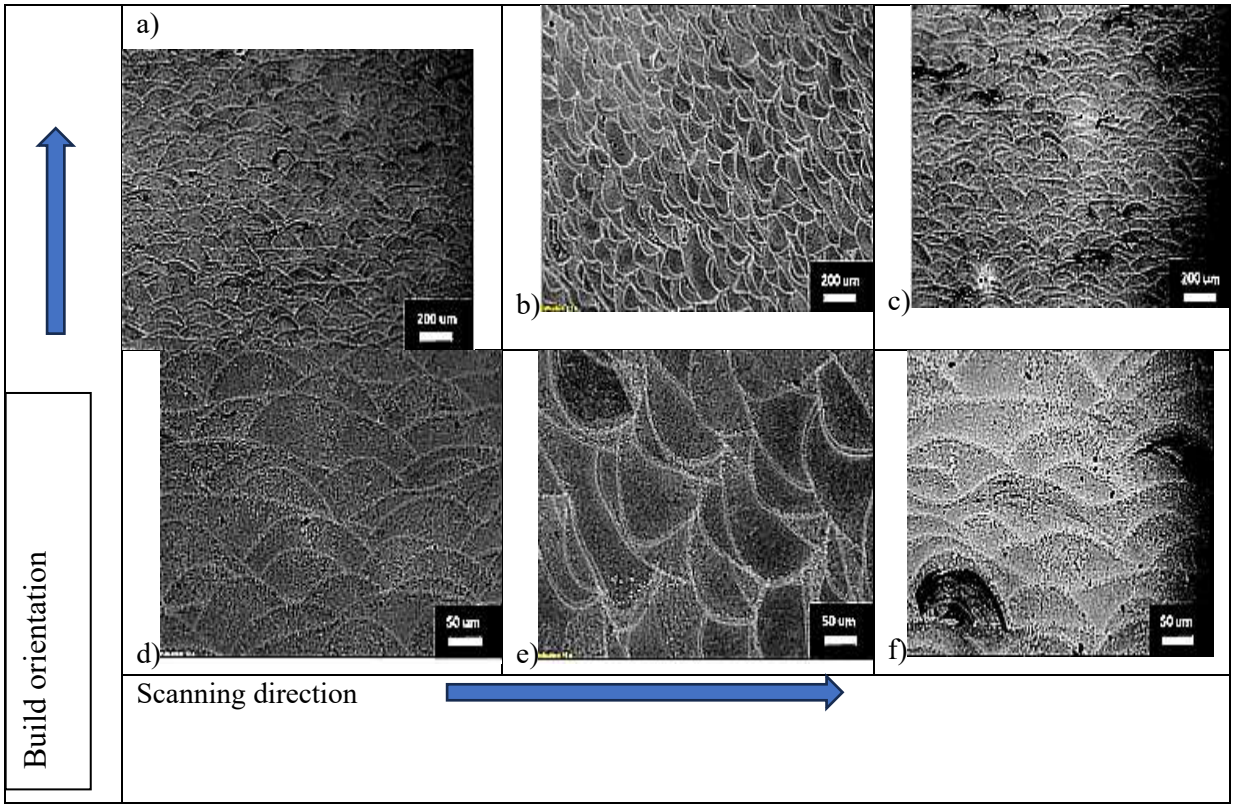

Figure 2. Microstructure of the SLM produced AlSi10Mg samples in various orientations, (a & d) XY, (b & e) 45°, and (c & f) Z orientations. (Images are presented at low and high magnifications, respectively)

3.3. Mechanical properties analysis

The hardness measurements are presented in Table 2, where the values obtained varied from 126–128 HV, which were relatively higher than previously reported values of 92 ± 5 HV for SLM-produced AlSi10Mg parts [3]. The hardness values were similar and showed only slight variation with changes in build orientation. Tensile tests were performed on the samples as shown in Figure 3 in order to determine the effect of build orientation on the mechanical properties of the fabricated parts. Typical stress–strain curves were obtained for all samples.

The elastic modulus for Batch A was 83 GPa, which was higher than the commonly reported elasticity of AlSi10Mg alloy (70 GPa) [5]. Elastic deformation was observed up to approximately 2.4 mm extension, withstanding stresses below 264 MPa before fracture occurred near 5 mm extension at stresses below 442 MPa.

The modulus of elasticity for Batch B was 82 GPa, which was also higher than commonly reported values. Elastic deformation was observed up to approximately 3.8 mm extension, withstanding stresses below 268 MPa before fracture occurred below 7 mm extension at stresses below 462 MPa. This behaviour may be associated with orientation-dependent porosity and weaker interlayer bonding characteristics. Previous investigations on porous aluminium alloys fabricated by additive manufacturing also reported unstable stress behaviour characterized by peaks and troughs during deformation [15]. The higher elastic modulus values observed for Batches A and B may be associated with residual stresses, localized densification effects, or experimental limitations associated with extension-based strain measurements during tensile testing.

The modulus of elasticity for Batch C was 71 GPa, which was close to the expected elasticity of AlSi10Mg alloy (70 GPa). Elastic behaviour was observed up to approximately 2 mm extension, withstanding stresses below 244 MPa before fracture occurred below 5 mm extension at stresses below 450 MPa.

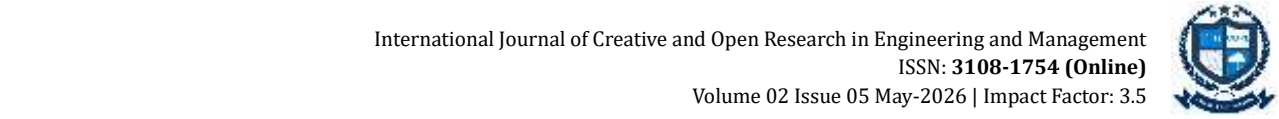

The average ultimate tensile strength (UTS) values obtained from triplicate measurements are presented in Figure 4a. The highest UTS was obtained for Batch C at 450 ± 6 MPa, while Batch A showed the lowest UTS value of 442 ± 4 MPa. These values are comparable to previously reported UTS values for selective laser sintering processed AlSi10Mg alloys (approximately 442 MPa) [5], and higher than stress-relieved SLM-produced AlSi10Mg alloys (272 MPa) [5] and cast A357 aluminium alloy (388 MPa) [5].

Figure 4b presents the elongation values obtained for different build orientations. Batch B exhibited the highest elongation of 7.4%, while Batch A showed the lowest elongation of 6.3%. These elongation values are slightly lower than previously reported stress-relieved SLM AlSi10Mg samples (8.5%) [5] but are comparable to heat-treated AlSi10Mg fabricated by SLM (6–9%) [3], and higher than die-cast A357 aluminium alloy (5.3%). In the present study, the highest ductility was obtained for Batch B corresponding to the 45° build orientation.

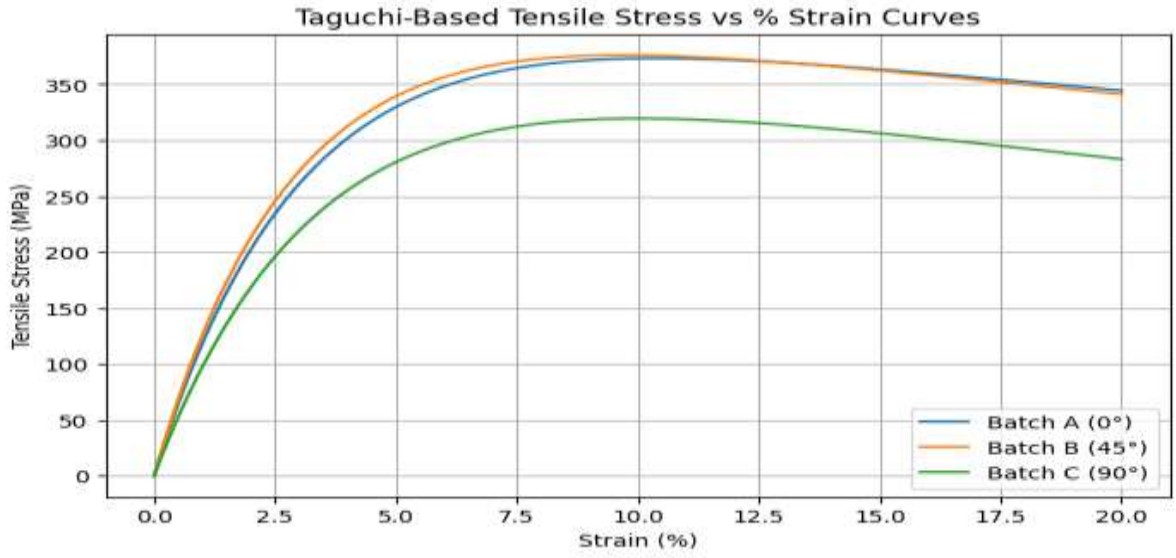

Figure 3. Stress-strain curves of the SLM produced AlSi10Mg samples at different build orientations

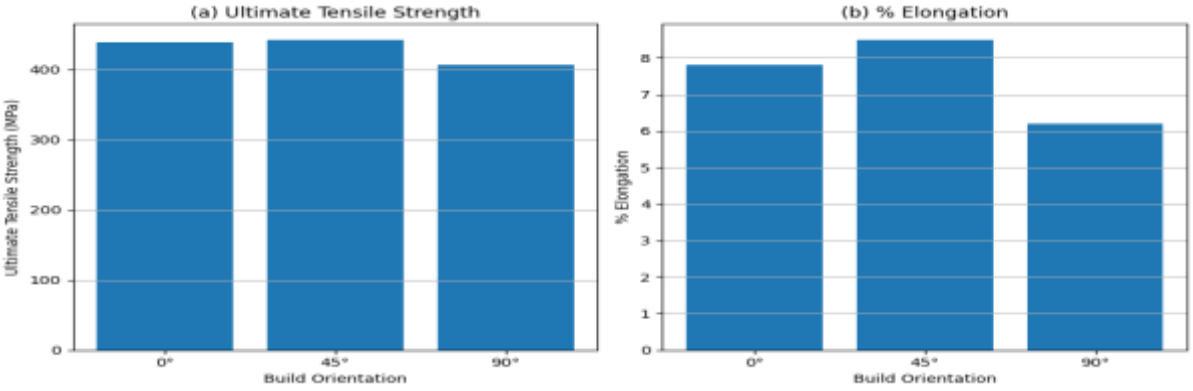

Figure 4. Tensile stress results of the SLM produced AlSi10Mg samples with build orientation and (a) ultimate tensile strength, and (b) % elongation.

4. Conclusions

The present study investigated the influence of build orientation on the density, microstructure, hardness, and tensile behaviour of SLM-fabricated AlSi10Mg alloy. The results demonstrated significant anisotropic mechanical behaviour associated with variations in build orientation. The XY-0° orientation exhibited the lowest porosity and relatively stable tensile behaviour, whereas the 45° orientation showed the highest ductility. The Z-90° orientation achieved the maximum ultimate tensile strength of 450 ± 6 MPa.

Microstructural analysis revealed characteristic melt pool morphologies, cellular-dendritic structures, and orientation-dependent pore distributions generated during the SLM process. The observed anisotropy was primarily attributed to differences in melt pool overlap, grain growth direction, and interlayer bonding characteristics. The findings confirm that build orientation plays a critical role in determining the mechanical performance of SLM-produced AlSi10Mg components and should therefore be carefully optimized according to specific engineering applications.

References

1. Thijs, L., Kempen, K., Kruth, J. P., & Van Humbeeck, J (2013). Fine-structured aluminium products with controllable texture by selective laser melting of pre-alloyed AlSi10Mg powder. *Acta Materialia, 61*(5), 1809–1819. https://doi.org/10.1016/j.actamat.2012.11.052
2. Read, N., Wang, W., Essa, K., & Attallah, M. M. (2015). Selective laser melting of AlSi10Mg alloy: Process optimisation and mechanical properties development. *Materials & Design, 65*, 417–424. https://doi.org/10.1016/j.matdes.2014.09.044
3. Kempen, K., Thijs, L., Van Humbeeck, J., & Kruth, J. P. (2012). Mechanical properties of AlSi10Mg produced by selective laser melting. *Physics Procedia, 39*, 439–446. https://doi.org/10.1016/j.phpro.2012.10.059
4. Brandl, E., Heckenberger, U., Holzinger, V., & Buchbinder, D. (2012). Additive manufactured AlSi10Mg samples using selective laser melting (SLM): Microstructure, high cycle fatigue, and fracture behavior. *Materials & Design, 34*, 159–169. https://doi.org/10.1016/j.matdes.2011.07.067
5. Vrancken, B., Thijs, L., Kruth, J. P., & Van Humbeeck, J. (2012). Heat treatment of selective laser melted AlSi10Mg to improve mechanical properties. *Journal of Alloys and Compounds, 541*, 177–185. https://doi.org/10.1016/j.jallcom.2012.07.022
6. Mertens, A., Reginster, S., Contrepois, Q., Dormal, J., & Lemaire, O. (2016). Microstructure and mechanical properties of selective laser melted AlSi10Mg in function of build orientation. *Physics Procedia, 83*, 882–889. https://doi.org/10.1016/j.phpro.2016.08.092
7. Ronneberg, T., Davies, M., & Hooper, P. A. (2020). Revealing relationships between porosity, microstructure and mechanical properties of selective laser melted AlSi10Mg parts. *Additive Manufacturing, 34*, 101265. https://doi.org/10.1016/j.addma.2020.101265
8. Wang, Y., Liu, H., & Zhang, J. (2023). Recent developments in selective laser melting of aluminium alloys: Process optimization and mechanical performance. *Materials Today Communications, 36*, 106512. https://doi.org/10.1016/j.mtcomm.2023.106512
9. Kruth, J. P., Levy, G., Klocke, F., & Childs, T. H. C. (2007). Consolidation phenomena in laser and powder-bed based layered manufacturing. *CIRP Annals, 56*(2), 730–759. https://doi.org/10.1016/j.cirp.2007.10.004
10. Wu, X., & Li, Y. (2023). Recent progress on the additive manufacturing of aluminum alloys and aluminum matrix composites: Microstructure, properties, and applications. *International Journal of Machine Tools and Manufacture, 190*, 104047. https://doi.org/10.1016/j.ijmachtools.2023.104047
11. Casati, R., & Vedani, M. (2022). Metal additive manufacturing: Processing, microstructure and anisotropic mechanical behavior of aluminum alloys. *Metals, 12*(6), 1024. https://doi.org/10.3390/met12061024
12. Kok, Y., Tan, X. P., Wang, P., Nai, M. L. S., Loh, N. H., Liu, E., & Tor, S. B. (2018). Anisotropy and heterogeneity of microstructure and mechanical properties in metal additive manufacturing: A critical review. *Materials & Design, 139*, 565–586. https://doi.org/10.1016/j.matdes.2017.11.021
13. Aboulkhair, S., Everitt, N., Ashcroft, I., & Tuck, C. (2014). Reducing porosity in AlSi10Mg parts processed by selective laser melting. *Additive Manufacturing, 1–4*, 77–86. https://doi.org/10.1016/j.addma.2014.08.001
14. Tang, M., & Pistorius, P. C. (2017). Oxides, porosity and fatigue performance of AlSi10Mg parts produced by selective laser melting. *International Journal of Fatigue, 94*, 192–201. https://doi.org/10.1016/j.ijfatigue.2016.06.002

15. Takata, A., Kodaira, N., Suzuki, A., & Kobashi, M. (2014). Mechanical properties of porous aluminum fabricated by additive manufacturing route. *Materials Science and Engineering: A, 613*, 287–294. https://doi.org/10.1016/j.msea.2014.06.099
16. DebRoy, T., Wei, H. L., Zuback, J. S., Mukherjee, T., Elmer, J. W., Milewski, J. O., Beese, A. M., Wilson-Heid, A., De, A., & Zhang, W. (2018). Additive manufacturing of metallic components – Process, structure and properties. *Progress in Materials Science, 92*, 112–224. https://doi.org/10.1016/j.pmatsci.2017.10.001
17. Qiu, C., Adkins, N. J. E., & Attallah, M. M. (2013). Microstructure and tensile properties of selectively laser-melted and of HIPed laser-melted AlSi10Mg. *Materials Science and Engineering: A, 578*, 230–239. https://doi.org/10.1016/j.msea.2013.04.092
18. Shaikh, J. B., Pathan, A., Borse, S. C., & Kolhapure, K. B. (2025). A review on lightweight materials for metal additive manufacturing process. *International Journal of Creative Research Thoughts (IJCRT), 13*(7), 120–133.